



Title	Hydrogen desorption behavior of aluminium materials used for extremely high vacuum chamber
Author(s)	Hirohata, Yuko; Fujimoto, Satoshi; Hino, Tomoaki; Yamashina, Toshiro
Citation	Journal of Vacuum Science & Technology A: Vacuum, Surfaces, and Films, 11(5), 2637-2641 https://doi.org/10.1116/1.578618
Issue Date	1993-09
Doc URL	http://hdl.handle.net/2115/5735
Type	article (author version)
File Information	JVS&TA-VSF11-5.pdf



[Instructions for use](#)

Hydrogen desorption behavior of aluminium materials used for extremely high vacuum chamber

Yuko Hirohata, Satoshi Fujimoto, Tomoaki Hino, and Toshiro Yamashina

Department of Nuclear Engineering, Faculty of Engineering, Hokkaido University, Kita-13, Nishi-8, Kita-ku, 060 Sapporo, Japan

(Received 14 December 1992; accepted 2 April 1993)

Hydrogen desorption properties of pure Al metal (1050H24 and 1001 Al) and Al alloy (6063T6) were investigated by using a technique of thermal desorption spectroscopy (TDS). In the TDS spectrum of hydrogen, two peaks in the temperature, which may correspond to the desorptions due to second-order surface reaction and diffusion process, were observed. The activation energy of the desorption, due to the surface reaction for the 1050H24 Al, was obtained as 38 kJ/mol. For the 1001 Al, by using a simple diffusion model, the activation energy and diffusion constant of hydrogen due to the diffusion process were calculated as 50 kJ/mol and $(0.5-3.5) \times 10^{-3} \text{ cm}^2/\text{s}$, respectively. The hydrogen desorption amount of the Al alloy was estimated as $3 \times 10^{15} \text{ mol/cm}^2$ (0.159 cc/100g Al), which was twice compared with that of the 1050H24 Al. Secondary-ion mass spectroscopy (SIMS) analysis was applied to examine the change of the surface atomic composition after baking. It was found that magnesium was considerably segregated by heating. However, the correlation between the concentrations of hydrogen and magnesium was not clearly observed.

I. INTRODUCTION

Aluminum or its alloys possess desirable characteristics, e.g., high thermal conductivity, low residual radioactivity, and low desorption rate of gases for numerous applications.^{1,2} Recently, the aluminium alloy or the aluminium metal has been used as an ultra high or extremely high vacuum chamber material.³⁻⁵ In the range of extremely high vacuum, the major residual gas species is hydrogen.^{6,7} Since the ultimate pressure is determined by the desorption rate of hydrogen from the chamber wall, thus it is important to understand the hydrogen desorption behavior of the aluminium or its alloy.

We, so far, have studied the activation energy of hydrogen desorption and the desorption amount from pure Al metal or Al alloy by using a technique of thermal desorption spectroscopy (TDS).⁶⁻⁸ In the present study we examined the activation energies of hydrogen desorption due to surface reaction and diffusion process. For the pure Al (1001A), we also estimated the diffusion rate of hydrogen by using a simple diffusion model.

In order to study the hydrogen concentration at the surface of Al metal or Al alloy, the secondary-ion mass spectroscopy (SIMS) technique was applied. The changes of the hydrogen and the magnesium concentrations due to baking were examined. The relation between the concentrations of hydrogen and magnesium after baking was also discussed.

II. EXPERIMENTAL

A TDS-SIMS combined system used in this work is schematically shown in Fig. 1. The system was evacuated both by a turbo molecular pump (TMP) and a Ti-sublimation pump. An orifice with a diameter of 10 mm was attached between the vacuum chamber and the pumping system. In this pumping system, a base pressure of

$1.0 \times 10^{-6} \text{ Pa}$ was achieved without baking. During a measurement of TDS spectrum, the chamber was evacuated only by the TMP. Effective pumping speed of the TMP for nitrogen (S_e) was obtained as $9.1 \times 10^{-3} \text{ m}^3/\text{s}$. Partial pressures and total pressure were measured by a quadrupole mass spectrometer (QMS) and a Bayard-Alpert (BA) gauge, respectively.

The sample was placed on a Ta heater by using a manipulator with a sample holder. It is possible to set five species on the sample holder. The Ta heater is resistively heated. The temperature was monitored by a chromel-alumel thermocouple spotwelded on the Ta heater. The sample was heated up to 500 °C according to two heating schemes (a) a linear increase of sample temperature, e.g., $BtT = T_0 + Bt$, in which heating rate, B , was changed from 3 to 30 °C/min, and (b) a constant heating temperature. Before and after the TDS measurement for the sample, the background spectrum was measured by heating only for the Ta heater.

Experiments were carried out for pure Al samples (1050H24, 1001) and Al alloy (6063T6) samples. Purities of 1050H24 and 1001 Al samples were 99.5% and 99.99%, respectively. Sample geometry was a slab strip of $12 \times 12 \times 1.2 \text{ mm}$. Before installation of the sample in the TDS apparatus, the sample was mechanically polished by using alumina powder, rinsed in ethanol in an ultrasonic bath, and dried in air at room temperature.

The SIMS technique was applied to examine the surface concentration of hydrogen. Ar^+ ion etching was used to measure the atomic depth composition. The energy and current density of the Ar^+ ions were 5 keV and 10^{-6} A/cm^2 , respectively. The Ar^+ ion beam was scanned for the region of $10 \times 10 \text{ mm}^2$. The etching rate of Al was estimated as about 2 nm/min from the sputtering data of Al.⁹

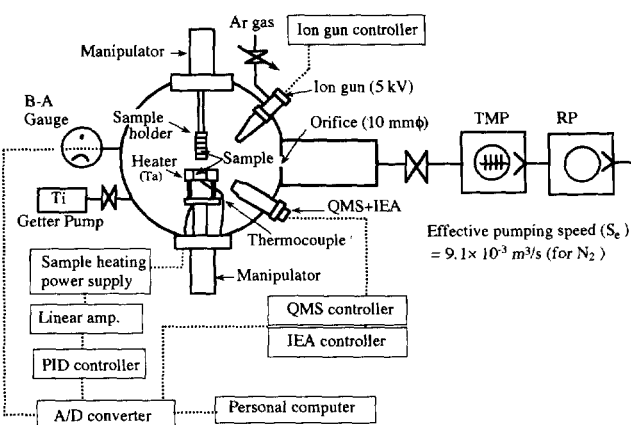


FIG. 1. Schematic diagram of a TDS-SIMS combined system.

III. RESULTS AND DISCUSSION

A. Activation energy of hydrogen desorption, and analysis of diffusion rate

Typical TDS spectra of 1050H24 Al are shown in Fig. 2. Major desorbed gas species were H_2 , H_2O , CO , CO_2 , and CH_4 . The total amount of desorbed hydrogen up to $500^\circ C$ was estimated as $(3-4) \times 10^{15}$ mol/cm², which corresponds to approximately half the total desorption amount of all the gas species.

Two peaks were observed in the TDS spectra except for CH_4 . From the data of the first peak with peak temperature of T_{p1} , the linearity for the determination of activation energy can be obtained, which will be shown later. Thus, it can be presumed that the first peak is due to the surface reaction of hydrogen atoms. For the second peak, no clear explanation on the process has been presented. In this article, we assume that the second peak is associated with diffusion of hydrogen from the bulk including the oxide layer. Figure 3 shows the plot of $\ln(T_{p1}^2/B)$ versus $1/T_{p1}$ for H_2 . Here, the data obtained in the same experimental series are indicated as Batch 1 or Batch 2. In spite of the

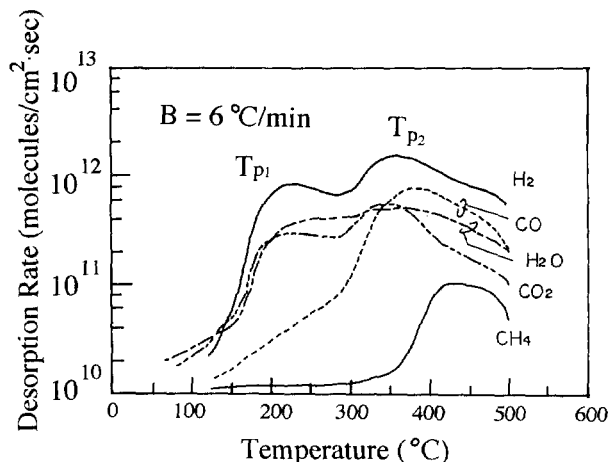
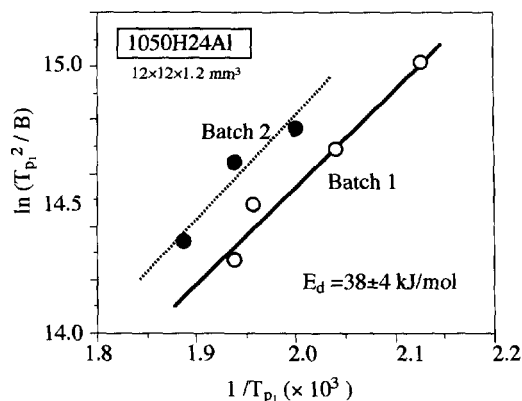
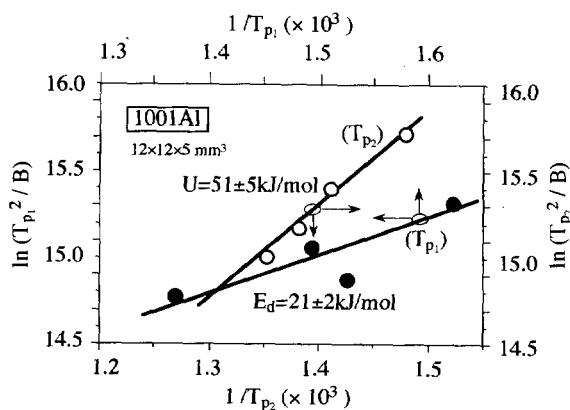


FIG. 2. Thermal desorption curve of pure Al metal (1050H24).

FIG. 3. Reciprocal peak temperature (T_{p1}) vs $\ln(T_{p1}^2/B)$.

same ramp rate, the value of peak temperature of T_{p1} varied when the experimental series was different. This result indicates that the desorption behavior due to the surface reaction limit is strongly affected by the surface state, such as diffusion, thickness or density of oxide layer, adsorbed species, or impurities, etc.^{8,10,11} However, for the first peak, the linearity between $\ln(T_{p1}^2/B)$ and $1/T_{p1}$ was found in the every experimental series (batch 1 or batch 2). The activation energy was obtained as 38.4 ± 4.0 kJ/mol from the slope of these straight lines. For the second peak, T_{p2} , it was difficult to find the linearity between $\ln(T_{p2}^2/B)$ and $1/T_{p2}$. This may be due to the difference of oxide layer in the samples. So, we investigated the hydrogen desorption behavior for 1001 Al whose purity is higher than that of 1050H24 Al. After polishing and rinsing, the sample of 1001 Al was immediately placed into the sample holder and was evacuated to reduce the effect of the formation of oxide layer. The sample geometry was $12 \times 12 \times 5$ mm.

Figure 4 shows the plot of $\ln(T_p^2/B)$ versus $1/T_p$ for H_2 . A linear relation between $\ln(T_p^2/B)$ and $1/T_p$ was found for both peaks, e.g., T_{p1} and T_{p2} . The activation energies for T_{p1} and T_{p2} were obtained as 21.2 ± 2 and

FIG. 4. Relation between $\ln(T_p^2/B)$ and $1/T_p$ for 1001 Al.

50 ± 5 kJ/mol, respectively. These values are approximately one-half of that previously reported for the 1060 Al.¹²

Since the desorption behavior of the second peak largely depends on the state of oxide layer, it may be presumed that the hydrogen desorption of the second peak is mainly due to diffusion from the bulk including the oxide layer. In the following we tried to calculate the diffusion rate based upon the obtained activation energy. For this purpose, we consider the following simple diffusion model.

When a sample is heated to a constant temperature, the desorption rate due to diffusion reaction limit, $q(t)$, in the case of a semi-infinite slab sample, is written by

$$q(t) = \frac{8C_0D}{d} \sum_0^{\infty} \exp\left[-\left(\frac{\pi(2n+1)}{d}\right)^2 Dt\right], \quad (1)$$

where C_0 and d are the initial concentration of hydrogen in an Al sample and the thickness of the slab sample, respectively. D is the diffusion constant. In the case of linear increase of sample temperature, D becomes a function of time, $D(t)$. Then, $D(t)$ is expressed as

$$D(t) = D_0 \exp\left(-\frac{U}{kT(t)}\right), \quad (2)$$

where U and D_0 are the activation energy of diffusion and a frequency factor, respectively. Since the distribution of the hydrogen concentration in Al varies with the heating time, the average value of $D(t)$ with respect to the heating time can be used for D in Eq. (1). The average value of $D(t)$ is defined by

$$Z(t) = \frac{1}{D_0} \int D(t) dt = \int \exp\left(-\frac{U}{kT}\right) dt. \quad (3)$$

When the sample temperature is lineally increased, $Z(t)$ is approximated as¹³

$$Z(t) \approx \frac{k}{BU} \left[T(t)^2 \exp\left(-\frac{U}{kT(t)}\right) - T_0^2 \exp\left(-\frac{U}{kT_0}\right) \right]. \quad (4)$$

In a case that the diffused hydrogen is immediately desorbed from the surface, the desorption rate becomes

$$q(t) = \frac{8C_0D}{d} \exp\left(-\frac{U}{k(T_0+Bt)}\right) \times \sum_0^{\infty} \exp\left[-\left(\frac{\pi(2n+1)}{d}\right)^2 \frac{D_0 k(T+Bt)^2}{BU}\right] \times \exp\left(-\frac{U}{k(T_0+Bt)}\right), \quad (5)$$

where the activation energy is assumed as a constant value.

Figure 5 shows the TDS spectra calculated from Eq. (5). Here, for U and D_0 , the values reported by Eichenauer¹⁴ were used. The peak temperature, T_p , shifted to the range of high temperature with an increase of B [Fig. 5(a)], but T_p was independent of C_0 [Fig. 5(b)]. In addition, the shape of the TDS spectrum became asymmetric with respect to T_p . From this calculation, it was found that the spectrum due to diffusion reaction limit became

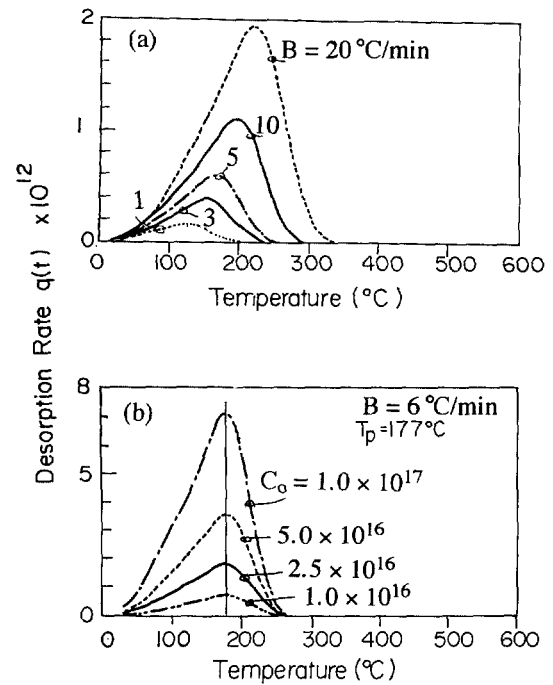


FIG. 5. TDS spectra calculated by using Eq. (5) for different ramp rate, B , and the initial concentration of hydrogen, C_0 . (a) $C_0 = 1 \times 10^{16}$ mol/cm³, $d = 0.1$ cm, $U = 40.92$ kJ/mol, $D_0 = 0.11$ cm²/s; (b) $d = 0.1$ cm, $U = 40.92$ kJ/mol, $D_0 = 0.11$ cm²/s, $B = 6$ °C/min.

similar to that of the surface reaction limit of first order reaction. We then obtained the activation energy of diffusion from a linear relationship between $\ln(T_p^2/B)$ and $1/T_p$, derived from Fig. 5(a). The activation energy obtained from the plot well agreed with the Eichenauer data. Thus we confirmed that the present model is self-consistent.

The activation energy of the diffusion for hydrogen experimentally observed was 50 ± 5 kJ/mol. The frequency factor, D_0 , became $(0.5-3.5) \times 10^{-3}$ cm²/s from the numerical simulation. In the simulation, U was assumed as constant (50 ± 5 kJ/mol) and D_0 be fitted to the peak temperature of the desorption. The value of the diffusion rate, D , experimentally obtained by numerous authors.¹⁵ The values for U and D_0 have the ranges from 40 to 60 kJ/mol, and from 10^{-3} to 1 cm²/s, respectively. The diffusion rate, D , at temperature of 100 °C has a wide range from 5.6×10^{-11} to 3.02×10^{-7} cm²/s. The present values for U and D_0 obtained in our experiment became similar, e.g., activation energy was 50 kJ/mol and diffusion rate at temperature of 100 °C was from 1.8×10^{-9} to 3.0×10^{-10} cm²/s.

B. Amount of desorbed hydrogen

Desorption spectra of hydrogen from the Al metal (1050H24) and the Al alloy (6063T6) at a constant temperature of 500 °C are shown in Fig. 6. The background spectra before and after the TDS experiment are also shown by dotted and broken lines, respectively. The desorption rate of hydrogen from the Al metal increased rap-

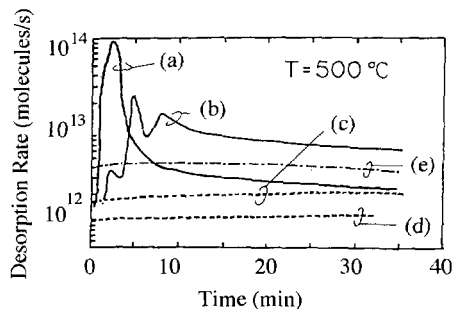


FIG. 6. Hydrogen desorption curves of 1050H24 Al, and 6063 Al alloy and the background. (a) TDS curve of 1050H24 Al, (b) TDS curve of 6063T6 Al alloy, (c) background of 1050H24 before and after heating, (d) background of 6063T6 before heating, (e) background of 6063T6 after heating.

idly within several minutes and after that continuously decreased. After 30 min, the desorption rate decreased to the background level.

Three peaks were observed in the spectrum of the Al alloy. The desorption rate of the 6063T6 Al was rather smaller than that of the 1050H24 Al in the initial heating phase, but even after heating for 30 min, the desorption rate did not approach the background level. After the TDS experiment of Al alloy, the background level became larger than that before the TDS experiment. This behavior, e.g., the appearance of three peaks and the enhancement of background level, may be caused by the formation of a Ta-Mg alloy on the surface of a Ta heater due to the evaporation of magnesium from the Al alloy. The Ta-Mg alloy is well known as a hydrogen-storage material. In order to obtain the amount of desorbed hydrogen from Al alloy, it is necessary to add the desorption amount of hydrogen from the Ta heater alone.

The total amount of hydrogen desorbed from the Al alloy was estimated as about 2.0×10^{16} mol (0.159 cc/100 g Al) by integrating the desorption spectrum with respect to time. This value was two times larger than that of 1050H24 Al. On the other hand, this value was one-half the value reported by Imabayashi (0.25 cc/100 g Al and Al alloy heated up to 700 °C)¹⁶ or by Kato (0.36 cc/100 g Al heated up to 900 °C).¹⁷ This difference may be explained,

TABLE I. The amount of desorbed hydrogen from pure Al and Al alloy samples.

Type	Pure Al samples		Al alloy sample
	1001	1050H24	6063T6
Desorption amount (cc/100 g Al)	0.04	0.088	0.159

because in the present experiment the temperature was not high enough for the Al to be melted and the heating time was not long enough for the hydrogen to be desorbed perfectly.

Table I shows the amount of hydrogen desorbed from pure Al and Al alloy during heating at a temperature of 500 °C for 30 min. It was found that the sample with a smallest amount of desorbed hydrogen was 1001 Al. The present data on the relationship between 6063T6 Al and 1050H24 Al at low temperature agrees with the data obtained by Chen and co-workers¹ and Narushima.¹²

C. Relation between surface concentrations of hydrogen and magnesium

For 6063T6 Al alloy and 1050H24 Al, SIMS analysis was applied to examine the change of surface composition. The SIMS spectra on the top surface and near surface region were shown in Fig. 7. The signal intensity of H^+ for Al alloy was larger than that of the Al metal both at the top surface and the region in the depth of about 240 nm. This result was consistent with the TDS data.

If Al alloy is used as a vacuum chamber material, the baking temperature must be kept lower than 150 °C because of low melting point of Al alloy. We then examined the change of surface composition of Al alloy during baking by using SIMS technique. Figure 8 shows the signal intensities of Mg^+ and H^+ for the 6063T6 Al alloy heated at a temperature 150 °C. The intensity of Mg^+ on the surface gradually increased with the heating time, about eight times enhanced compared with the case before heating. The thickness of the alternated layer was roughly 60 nm.

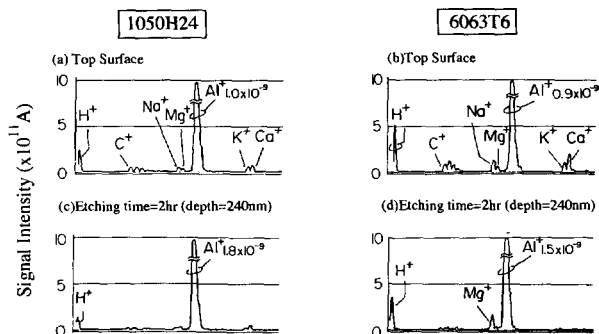


FIG. 7. SIMS spectra of 1050H24 Al and 6063T6 Al alloy before and after etching with Ar^+ ion.

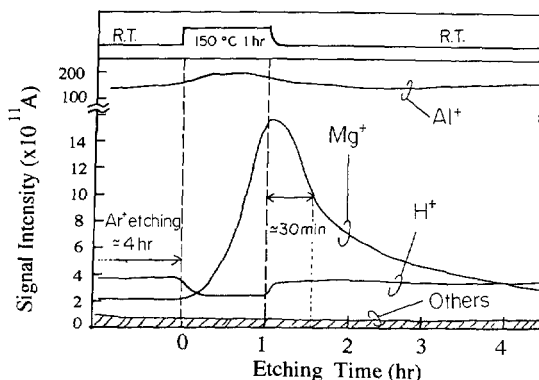


FIG. 8. Surface analysis of 6063T6 Al alloy heated at 150 °C and cooled at room temperature during Ar^+ ion etching.

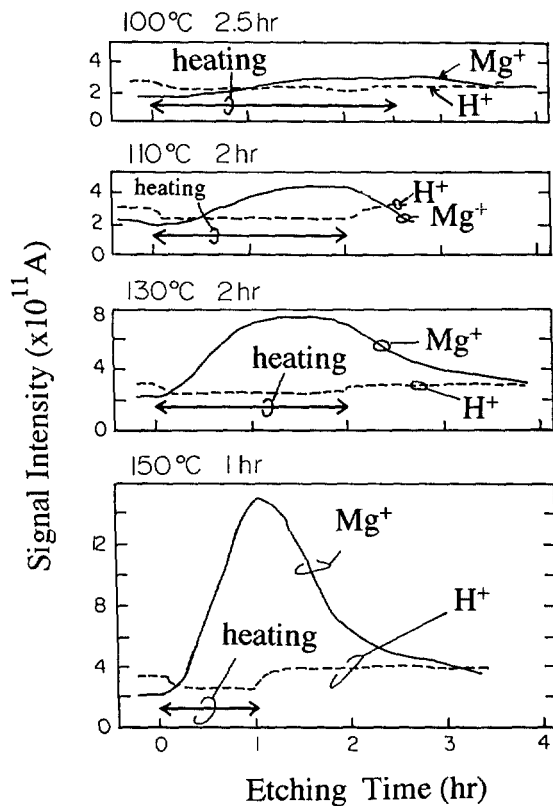


FIG. 9. Changes of SIMS signal intensities of Mg^+ and H^+ with different heating conditions.

The signal intensity of H^+ became small during heating, but after heating it returned to the previous level. Figure 9 shows the signal intensities of Mg^+ and H^+ of Al alloy heated at different heating conditions. The segregation of Mg became large with increase of the heating temperature. The ratio of signal intensities of H^+ to Al^+ was almost the same for each baking schedule. The hydrogen concentration on the surface was observed to be independent of the magnesium concentration. It can be assumed that the amount of hydrogen on the surface due to readsorption is already saturated, since the hydrogen amount did not increase with magnesium concentration.

IV. CONCLUSION

A TDS technique was applied to investigate the hydrogen desorption behavior of Al materials. The amount of H_2 desorbed from the Al alloy during heating at $500^\circ C$ for 30 min became 0.159 cc/100 g, which was twice and four times larger than those of 1050H24 Al and 1001 Al, respectively. The activation energy of desorbed hydrogen due to the hydrogen recombination was estimated as 38.4 ± 4 kJ/mol for the 1050H24 Al. For the 1001 Al sample, the diffusion rate was obtained as $D = (0.5-3.5) \times 10^{-3} \exp [50 \pm 5 \text{ (kJ/mol)}/RT]$ (cm^2/s) by using a simple diffusion model.

The segregation of magnesium became dominant during the baking at temperature of $150^\circ C$. However, the concentration of magnesium in the surface had no relation to the surface concentration of hydrogen. In present experimental condition, it is presumed that the magnesium has no gettering action for hydrogen.

ACKNOWLEDGMENT

The authors wish to thank the Light Metal Foundation in Japan for their financial support of this work.

- ¹J. R. Chen, K. Narushima, and H. Ishimaru, *J. Vac. Sci. Technol. A* **3**, 2188 (1985).
- ²S. Ueda, Y. Ishikawa, and H. Kamohara, *Jpn. J. Vac. Soc.* **31**, 976 (1988).
- ³H. Ishimaru, K. Narushima, K. Kanazawa, and Y. Suetsugu, *J. Vac. Sci. Technol. A* **6**, 1293 (1988); H. Ishimaru, *ibid.* **7**, 2439 (1989).
- ⁴T. Kikuchi and S. Ohsako, *Jpn. J. Vac. Soc.* **33**, 72 (1990).
- ⁵A. G. Mathewson, J.-P. Bacher, K. Booth, R. S. Calder, G. Dominichini, A. Grillot, N. Hilleret, D. Latorre, F. LeNormand, and W. Unterlerchner, *J. Vac. Sci. Technol. A* **7**, 77 (1989).
- ⁶P. Redhead, *Vacuum* **12**, 203 (1962).
- ⁷G. Carter, *Vacuum* **12**, 245 (1962).
- ⁸T. Tai, Y. Muroo, and O. Konno, *Japan J. Vac. Soc.* **33**, 514 (1990).
- ⁹K. Tsunogaya, T. Suzuki, Y. Ohashi, and H. Kishidaka, *Surf. Interface Anal.* **2**, 212 (1980).
- ¹⁰Y. Kato, E. Isoyama, and M. Hasegawa, *Jpn. J. Light Metals* **38**, 462 (1988).
- ¹¹Y. Hirohata, M. Hashiba, T. Hino, and T. Yamashina, *Bull. Fac. Eng. Hokaido Univ.* No. 158 71 (1992), No. 159 19 (1992).
- ¹²K. Narushima and H. Ishimaru, *Jpn. J. Vac. Soc.* **26**, 353 (1983).
- ¹³Y. Hirohata, *Jpn. J. Vac. Soc.* **33**, 488 (1990).
- ¹⁴W. Eichenauer and A. Pebler, *Z. Metall.* **48**, 373 (1957).
- ¹⁵K. Watanabe, K. Ashida, and M. Sonobe, *J. Nucl. Mater.* **173**, 294 (1990).
- ¹⁶M. Imabayashi, *Jpn. J. Light Metals* **23**, 38 (1973).
- ¹⁷Y. Kato, T. Kitamura, E. Isoyama, and M. Hasegawa, *J. Vac. Sci. Technol. A* **6**, 3111 (1988).